JOURNAL OF PROPULSION AND POWER
Vol. 15, No. 6, November–December 1999

Effect of Melting on Dynamic Combustion Behavior of Energetic Materials

L. K. Gusachenko* and V. E. Zarko†
Institute of Chemical Kinetics and Combustion, 630090, Novosibirsk, Russia
and
A. D. Rychkov‡
Institute of Computational Technologies, 630090, Novosibirsk, Russia

The effect of melting on the intrinsic stability of steady-state combustion of energetic materials has been analytically studied using the Zeldovich–Novozhilov approach. Stability limits are given in conventional and modified sensitivity parameters coordinates. Their dependence on the melting heat and temperature is explained in a simple way. Numerical calculations based on an original mathematical model were performed to verify the effects of melting on the stability of pressure-driven combustion regimes. Qualitatively, the effect of melting heat on the stability of transient combustion regimes with developed gas phase reactions is the same as that on the stability of steady-state regime, that is, as the melting heat increases, the stability decreases. In addition, the effect of melting temperature on the burning rate response to harmonic pressure oscillations has been numerically studied. The effect appears to be qualitatively the same under stationary and transient regimes, that is, as the melting temperature increases and approaches the temperature of the burning surface, the response function decreases noticeably in its absolute value, which corresponds to an increase of combustion stability.

Nomenclature

A_{gi} = pre-exponential factor for ith gas phase reaction, g/(cm$^3\cdot$ s $\cdot$ atm^{N_i})
A_{liq} = pre-exponential factor for condensed phase reaction, 1/s
C = specific heat, cal/(g $\cdot$ K)
C_{pi} = constant-pressure heat capacity of species i, cal/(g $\cdot$ K)
D = diffusion coefficient, cm^2/s
E = energy of activation, cal/mol
f = frequency of oscillations, 1/s
k = dimensionless parameter, identical to $(T_s - T_0)(\partial \ln r_b/\partial T_0)_p$
L = latent heat of evaporation, cal/g
M_i = molecular mass of species i, g/mol
m^* = mass flow rate of condensed phase, g/cm^2 s
N = gas reaction order
p = pressure, atm
p_0 = atmospheric pressure, atm
Q = heat release per unit mass, cal/g
q_r = radiant flux, cal/(cm^2 s)
R = universal gas constant, cal/(mol $\cdot$ K)
r = dimensionless parameter, identical to $[\partial T_s/\partial T_0]_p$
r_b = burning rate, cm/s
T = temperature, K
T_b = boiling temperature at atmospheric pressure, K
t = time, s
V = gas velocity, cm/s
V_{liq} = liquid velocity, cm/s
V_m = velocity of solid/liquid interface, cm/s
x = spatial coordinate, cm
x_{tw} = characteristic distance for thermal wave decay in condensed phase, cm
y_i = mass fraction of specie i
α = extinction coefficient in the Beer law, 1/cm
β = porosity (volumetric fraction of gas)
λ = thermal conductivity, cal/(cm s $\cdot$ K)
ρ = density, g/cm^3
ω = dimensionless frequency of oscillations

Subscripts

liq = parameters of the liquid state
m = melting
s = propellant surface
sol = parameters of the solid state
0 = initial condition
1, 2, 3 = vapor, intermediate, and final reaction products, respectively

I. Introduction

IT is known that many energetic materials (EMs) melt in a combustion wave and have a liquid layer on the burning surface. In addition, the EMs may change their crystal structure at a relatively low temperature. Typically, in stationary combustion modeling, the effects of phase changes are taken into account in a very simple way by introducing the effective initial temperature calculated on the basis of heat balance at the burning surface.[1]

However, when modeling transient combustion, it is not clear a priori if the effect of phase changes can be explained as simply. One may expect that the transient combustion behavior of EMs, at least near the limits of the combustion stability, depends on the heat and temperature of phase transitions. Obviously, the highest effect is produced by evaporation that is localized at the surface of the condensed phase and has, as a rule, the largest magnitude of the latent heat. In the past, mainly the evaporation was considered in combustion modeling. Nevertheless, it seems that the effect of other phase transitions also should be studied, and attempts to explore this problem have been undertaken in recent works.[2–4] It was shown that melting or phase transition, whose latent heat is considerably less than that of evaporation, may play a specific role in radiation-driven combustion,[2] as well as in the intrinsic stability of EM combustion.[3,4]

The cited works have dealt mainly with an analytical approach, and it is of interest to investigate numerically the combustion behavior of a melted EM in transient regimes using a mathematical

Received 4 February 1998; revision received 27 April 1999; accepted for publication 30 April 1999.

*Leading Scientist, Laboratory of Condensed Systems Combustion.
†Head, Laboratory of Condensed Systems Combustion. Associate Fellow AIAA.
‡Leading Scientist, Laboratory of Numerical Analysis.

model. In the present paper the effect of melting heat and melting temperature on the stability of pressure-driven combustion has been studied. The combustion model is presented in Sec. II. The results of the analytical study of intrinsic stability of combustion are presented in Sec. III. Burning rate response to harmonic variations of pressure is described in Sec. IV. Conclusions and future plans are given in Sec. V.

II. Mathematical Model

A. General Description

A model is proposed to describe combustion of melted and evaporated EM with chemical transformations in the condensed and gas phases. Typical representatives of such EMs are nitramines, as well as newly synthesized oxidizers such as ADN, HNF, etc.

In the condensed phase the model considers heat propagation in solid and liquid states (heat capacity and density are taken to be the same for both of the states whereas thermal conductivity coefficients for solids and liquids are assumed to be different), melting at temperature T_m with endothermal effect Q_m with a global exothermic reaction of decomposition of first order in the liquid phase with a thermal effect Q_{liq} and radiation absorption in the bulk of condensed phase according to the Beer law, $q_r \alpha e^{-\alpha x}$. The absorption coefficient α is taken to be the same for solid and liquid materials. The interface between the solid and the liquid states moves through the condensed phase with velocity V_m.

In the gas phase the model takes into account heat propagation, diffusion, and two global reactions with thermal effects Q_i, $i = 1, 2$. The products of the first reaction (vapor decomposition via N_1-order kinetics, mainly of first order) are assumed to coincide in their composition with the products of decomposition of the liquid phase. The second reaction generates final combustion products via N_2-order kinetics. Reaction routes of the combustion process are presented by the scheme

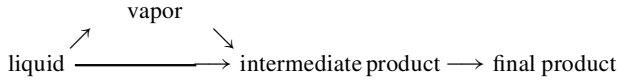

The choice of proper reaction scheme is a very complicated task and still has insufficient background. This is of special concern with the reactions in the condensed phase. Attempts have been made to formulate a reaction scheme consisting of several (up to seven) global reactions,[5,6] but there is still no real justification for that. Evidently, when using a global reaction approach, one has to describe the method for the experimental determination of kinetic parameters.

In the present work, the constants for condensed phase reaction were estimated on the basis of literature data for thermal decomposition of nitramines.[7] In fact, this is a very crude estimate because of the great difference in the heating rate for combustion and thermal decomposition conditions. In the future we plan to obtain the needed data from experiments on ignition under special conditions that provide the elimination of the possible effects of the gas phase reactions.

In the literature several detailed schemes for flame reactions in nitramines combustion,[8–11] containing more than 40 species and more than 200 steps, may be found. Use of such schemes allows, in principle, the calculation of temperature and concentration profiles in flame. Unfortunately, the use of the detailed reaction schemes causes difficulties in the calculation of transient regimes, and it is reasonable to derive reduced kinetic schemes for studying dynamic combustion behavior. This is a task for future work. At the same time, the global kinetic parameters can be derived from the treatment of experimental data of combustion of melted EMs in well-characterized conditions. To do that, a set of calculations on the basis of the model should be performed. As a first estimate, the data for thermal decomposition of nitramines vapor and the reaction between their products were used in the present work to specify the magnitude of global kinetic parameters for the gas phase reactions.

B. Physical State of the Condensed Phase

Before formulation of the mathematical model, it is important to discuss physical aspects regarding the processes in the bulk and on the surface of the condensed phase. Presence of the chemical reactions in the bulk of the condensed phase raises questions on the effective density of liquid EMs and on the evolution of the gas through the subsurface layer. It is natural to assume that gaseous decomposition products first dissolve in the liquid layer.[12] However, if one takes into consideration an equilibrium solution of gas in the liquid material this corresponds to a negligibly small extent of EM decomposition in the condensed phase.[13] At the finite decomposition degree one may assume that the gas bubbles form in the liquid layer. Their behavior can be described in several ways.

A first description was suggested in 1966,[14] when it was assumed that the velocities of gas and liquid are the same, $V = V_{\text{liq}} = m^*/\rho_c$. Here, $\rho_c = (1-\beta)\rho_{\text{liq}} + \beta\rho$ is the effective density of the condensed phase. More detailed analyses of two-phase subsurface layer were reported in Refs. 15–17. In particular, semi-empirical expressions were suggested[16] in the general case for linear velocity of gas motion $V = (1 - s\beta + s)m^*/\rho$ and liquid motion $V_{\text{liq}} = (1 - s\beta)m^*/\rho_{\text{liq}}$, respectively. Here s is the matching parameter varying in the range from zero to infinity that allows us to describe extreme cases of gas release from subsurface layer.

In the present model we consider the simplest case of constant density over the liquid layer. This corresponds to the case of gases dissolved in liquid without formation of bubbles or the case of instantaneous ($V \to \infty$ and $s \to \infty$) removal of gas out of the liquid layer. Note that, for very thin layers, diffusion is also able to provide fast removal of gas from liquid. To estimate, let us assume that gaseous products start to evolve in the bulk of the EMs at the distance from the surface equal to the length of reaction zone, $l_{ch} \approx 0.1(\lambda/C\rho)_{\text{liq}}/r_b$. If the residence time for liquid in the reaction zone, l_{ch}/r_b, is greater than the diffusion time $(l_{ch})^2/D$, where D is the diffusion coefficient, the bubbles will not form.

The described condition is formulated as $D(T_s) > r_b l_{ch} = 0.1(\lambda/C\rho)_{\text{liq}}$. A simple estimate shows that the condition approximately holds for typical melted EMs with $D \geq 10^{-4}$ cm^2/s and $(\lambda/c\rho)_{\text{liq}} = 0.001$ cm^2/s.

Detailed consideration of the effect of bubbles on the heat transfer across the liquid layer due to internal evaporation within the bubbles and of the Marangoni and Archimed effects was not made in the present paper. There are still no reliable observations of foam in subsurface liquid layer of burning melted EMs. Quite the contrary, observations have been reported[18] of the virtual absence of developed foam at the burning surface of double-base propellants at atmospheric and elevated pressures despite the presence of foam at the surface of extinguished samples. Thus, introduction of bubbles formation into comprehensive combustion models has to be justified by unambiguous experimental findings. One of the ways to get such information is to perform high-speed movie studies of EM combustion with use of a soft x-ray radiation source.

C. Surface Evaporation Condition

As mentioned, according to the model conversion of the condensed phase into gas proceeds by the way of chemical reaction and evaporation. The latter can be precisely described in terms of gas-kinetic theory if one calculates the mass flow rates of evaporation and condensation. Under nonequilibrium conditions, corresponding to the combustion process, the difference between the two rates gives mass burning rate. Such an approach has been employed in several works[8–10,16]; however, it is rather difficult to use this approach in real calculations. First, there is no reliable knowledge of the sticking coefficient that characterizes the sticking of vapor molecules colliding the liquid/gas interface. Second, and most important, the difference between the two rates represents the difference between two large quantities, and a small error in their calculation leads to a large error in the mass burning rate.

Therefore, in the present model we use another description based on that the deviation of the partial pressure of vapor from its equilibrium value is of the order of the Mach number for combustion products, with the magnitude of this number being much less than unity. Consequently, as was suggested in Ref. 19, one may approximately attribute the real magnitude of the vapor pressure to its

equilibrium value, which can be easily calculated on the basis of the Clausius–Clapeyron equation in the form

$$(M/M_1)y_{1s}p \sim \text{const}\cdot\exp(-L/RT_s)$$

where $(M/M_1)y_{1s}$ is the mole fraction of vapor above the surface and p is the ambient pressure. Use of this equation provides a better opportunity for convergence of the iteration process in numerical modeling. Note that, in the gas-kinetic approach, the Clausius–Clapeyron equation is also used for calculating the equilibrium pressure of vapor. The accuracy of these calculations directly depends on the accuracy of the value of the latent heat of vaporization. Unfortunately, for real EMs, this value is known with rather low accuracy because of the partial decomposition of the EMs at relatively high temperatures. The heat of vaporization can be calculated[20] on the basis of semi-empirical expressions or can be determined by extrapolation of data of surface temperature measurement.

D. Problem Formulation

Let us choose a movable coordinate system (x, t) attached to the burning surface (positive x axis is directed in the bulk of the condensed material) and derive the system of equations describing the physicochemical processes in the condensed phase.

For the solid state $[x_m(t) \le x \le x_R]$,

$$C_{\text{sol}}\rho_{\text{sol}}\left(\frac{\partial T_{\text{sol}}}{\partial t} - r_b\frac{\partial T_{\text{sol}}}{\partial x}\right) = \lambda_{\text{sol}}\frac{\partial^2 T_{\text{sol}}}{\partial x^2} + q_r(t)\alpha\exp(-\alpha x)$$

$$T_{\text{sol}}(x,0) = T_0, \qquad T_{\text{sol}}(x_m,t) = T_m, \quad \text{at} \quad x = x_R \qquad \frac{\partial T_{\text{sol}}}{\partial x} = 0$$

For the liquid state $(0 \le x \le x_m)$,

$$C_{\text{liq}}\rho_{\text{liq}}\left(\frac{\partial T_{\text{liq}}}{\partial t} - r_b\frac{\partial T_{\text{liq}}}{\partial x}\right) = \lambda_{\text{liq}}\frac{\partial^2 T_{\text{liq}}}{\partial x^2} + \Phi_{\text{liq}} + q_r(t)\alpha\exp(-\alpha x)$$

$$\rho_{\text{liq}}\left(\frac{\partial y_{\text{liq}}}{\partial t} - r_b\frac{\partial y_{\text{liq}}}{\partial x}\right) = -\omega_{\text{liq}}, \qquad \Phi_{\text{liq}} = Q_{\text{liq}}\omega_{\text{liq}}$$

$$\omega_{\text{liq}} = A_{\text{liq}}\rho_{\text{liq}}y_{\text{liq}}\exp\left(-\frac{E_{\text{liq}}}{RT_{\text{liq}}}\right), \qquad y_{\text{liq}}(x_m,t) = 1$$

$$T_{\text{liq}}(x,0) = T_0, \qquad T_{\text{liq}}(x_m,t) = T_m$$

$$-\lambda_{\text{liq}}\left.\frac{\partial T_{\text{liq}}}{\partial x}\right|_{x=x_m-0} = -\lambda_{\text{sol}}\left.\frac{\partial T_{\text{sol}}}{\partial x}\right|_{x=x_m+0} + Q_m V_m\rho_{\text{liq}}$$

(Note that variables without an index correspond to the bulk of gas.) The condensed phase generates vapor and a combustible gas. Thus, there are three components in the gas phase: vapor, intermediate decomposition product, and final combustion product. The temperature of the components is uniform at the given point of space.

The system of equations for the gas phase is as follows $(x_L \le x \le 0)$:

$$C_p\rho\left[\frac{\partial T}{\partial t} + \left(V - r_b - \sum_{i=1}^{3}\frac{C_{pi}}{C_p}D_i\frac{\partial y_i}{\partial x}\right)\frac{\partial T}{\partial x}\right] = \frac{\partial}{\partial x}\left(\lambda\frac{\partial T}{\partial x}\right) + \Phi_1 + \Phi_2$$

$$\rho\left[\frac{\partial y_1}{\partial t} + (V - r_b)\frac{\partial y_1}{\partial x}\right] = \frac{\partial}{\partial x}\left(\rho D_1\frac{\partial y_1}{\partial x}\right) - \omega_1$$

$$\rho\left[\frac{\partial y_2}{\partial t} + (V - r_b)\frac{\partial y_2}{\partial x}\right] = \frac{\partial}{\partial x}\left(\rho D_2\frac{\partial y_2}{\partial x}\right) - \omega_2 + \omega_1$$

$$\frac{\partial\rho}{\partial t} - r_b\frac{\partial\rho}{\partial x} + \frac{\partial(\rho V)}{\partial x} = 0, \qquad p = \frac{R\rho T}{M}$$

$$\frac{1}{M} = \frac{y_1}{M_1} + \frac{y_2}{M_2} + \frac{y_3}{M_3}, \qquad \Phi_1 = Q_1\omega_1$$

$$\Phi_2 = Q_2\omega_2, \qquad \omega_1 = A_{g1}(p\quad y_1)^{N_1}\exp\left(-\frac{E_1}{RT}\right)$$

$$\omega_2 = A_{g2}(p\quad y_2)^{N_2}\exp\left(-\frac{E_2}{RT}\right), \qquad T(x,0) = T_0$$

$$y_1(x,0) = y_2(x,0) = 0$$

$$\frac{\partial T}{\partial x} = \frac{\partial y_1}{\partial x} = \frac{\partial y_2}{\partial x} = 0, \qquad \text{at} \quad x = x_L$$

Boundary conditions at $x = 0$ are taken in the form

$$\lambda\left.\frac{\partial T}{\partial x}\right|_{x=-0} = \lambda_{\text{liq}}\left.\frac{\partial T_{\text{liq}}}{\partial x}\right|_{x=+0} - y_{\text{liq},s}\rho_{\text{liq}}r_bL$$

$$-\rho(V - r_b)y_{1s} + D_1\rho\frac{\partial y_1}{\partial x} = y_{\text{liq},s}\rho_{\text{liq}}r_b$$

$$-\rho(V - r_b)y_{2s} + D_2\rho\frac{\partial y_2}{\partial x} = \rho_{\text{liq}}r_b(1 - y_{\text{liq},s})$$

$$\rho(V - r_b) = -\rho_{\text{liq}}r_b$$

$$\frac{p}{p_0}y_{1s} = \frac{M_1}{M}\exp\left[-\frac{LM_1}{R}\left(\frac{1}{T_s} - \frac{1}{T_b}\right)\right]$$

In the case of opaque material $(\alpha \to \infty)$, the term with q_r must be withdrawn from thermal conductivity equations for solid and liquid phases, and the boundary condition for the heat fluxes should be written in the form

$$\lambda\left.\frac{\partial T}{\partial x}\right|_{x=-0} = \lambda_{\text{liq}}\left.\frac{\partial T_{\text{liq}}}{\partial x}\right|_{x=+0} + q_r - y_{\text{liq},s}\rho_{\text{liq}}r_bL$$

The mass fraction of the combustion product and its effective diffusion coefficient are determined on the basis of the mass conservation equation and the condition of zero sum of the individual mass diffusion fluxes,

$$D_1\frac{\partial y_1}{\partial x} + D_2\frac{\partial y_2}{\partial x} + D_3\frac{\partial y_3}{\partial x} = 0, \qquad y_1 + y_2 + y_3 = 1$$

E. Numerical Method

The equations of energy and species concentrations in the gas phase include convective and diffusive terms. It is known that there exist computational difficulties in their solution when using central-difference schemes for the convective term. Another difficulty is the stiffness of the equations. To overcome these difficulties, a quasi-monotonous difference scheme of second-order accuracy has been developed that effectively operates on real difference grids. Its essence may be explained by taking as an example the model nonlinear equation for a scalar function ϕ in domain $G\{0 \le x \le 1, 0 \le t \le T\}$,

$$\frac{\partial\phi}{\partial t} + u\frac{\partial\phi}{\partial x} = a\frac{\partial^2\phi}{\partial x^2} + f(\phi,t) \tag{1}$$

where u is the velocity, a is the constant, and $f(\phi, t)$ is the source term. The use of approximation $\partial\phi/\partial x \approx (\phi_{i+1}^{n+1} - \phi_{i-1}^{n+1})/(2h)$ for the convective term leads to the nonphysical oscillations appearing in the numerical solution in the range of a sharp change of value ϕ. For a given class of problems this corresponds usually to the reaction zone, where the temperature and concentration gradients are high enough. To eliminate these oscillations one may apply a difference scheme based on hyperbolic approximation. To this end we wrote the left-hand side of Eq. (1) along line $dx/dt = u$, which is conventionally called the characteristic line, and constructed the following

nonlinear two-step difference scheme using backward Tailor-series expansion of the term $f(\phi, t)$ in time:

$$\frac{\tilde{\phi}_i^{n+1} - \phi_*^n}{\tau} = a_*^n \left(\frac{\partial^2 \tilde{\phi}}{\partial x^2} \right)_i^{n+1} + f(\tilde{\phi}, t+\tau)_i^{n+1} \tag{2}$$

$$\frac{\phi_i^{n+1} - \phi_*^n}{\tau} = 0.5 \times \left[a_i^n \left(\frac{\partial^2 \phi}{\partial x^2} \right)_i^{n+1} + a_*^n \left(\frac{\partial^2 \phi}{\partial x^2} \right)_*^n \right] + f(\phi, t+\tau)_i^{n+1} \left[1 + \frac{\tau}{2} \left(\frac{\partial \tilde{f}}{\partial \phi} \right)_i^{n+1} \right] \tag{3}$$

where τ and h are the grid steps over the spatial and time variables so that $t = n\tau$; $x = ih$; $n = 0, \ldots, 1/h$; $i = 0, \ldots, T/\tau$. The values with subscript asterisks are calculated using appropriate interpolations at the cross points of the characteristic lines starting from the point $(n+1, i)$ with the straight lines forming the difference grid (with the horizontal ones at $h/\tau > u$ and with the vertical ones at $h/\tau < u$). The nonlinear difference scheme Eqs. (2) and (3) can be easily solved by the Newton method.

Now returning to the solution of the original problem formulation, the following procedure has been used. The surface temperature T_s and the burning rate r_b were found via an inner iteration procedure at each time-marching step. For a given initial guess of T_s and r_b, the equations for species concentrations were solved. Then values y_{1s}, y_{2s}, and $y_{\mathrm{liq},s}$ were used to determine the boundary conditions for the energy equations in the gas and condensed phase. After solution of the energy equations, new values of T_s and r_b were found from boundary conditions. The inner loop was repeated down to the convergence of T_s and r_b. A variable step grid, condensed in the vicinity of the liquid/gas interface, was used to get the results with 0.1% accuracy.

To solve numerically the problem with closing initial and boundary conditions, a spatial domain $x_L < x < x_R$ has to be chosen on the basis of physical considerations or numerical experiment. The domain size should allow us to establish zero gradients of temperature and species concentrations on the boundaries.

For the gaseous mixture, the corresponding diffusion coefficients were calculated using the Wilke formula: $1/D_i = y_1/D_{i1} + y_2/D_{i2} + y_3/D_{i3}$. Values of D_{ik} were calculated using the Lennard–Jones potential with $(\varepsilon/k)_1 = 436$ K, $(\varepsilon/k)_2 = 244$ K, and $(\varepsilon/k)_3 = 97$ K and $\sigma_1 = 6\,A^o$, $\sigma_2 = 3.7\,A^o$, and $\sigma_3 = 3.6\,A^o$. The thermal conductivity and specific heat of the gaseous mixture were calculated by the formulas $\lambda = \lambda_1 y_1 + \lambda_2 y_2 + \lambda_3 (1 - y_1 - y_2)$, $c = c_1 y_1 + c_2 y_2 + c_3 (1 - y_1 - y_2)$, $\lambda_i = A_{\lambda i} + B_{\lambda i} T$, $c_i = A_{ci} + B_{ci} T$, $A_{\lambda i} = 5 \times 10^{-5}$, 8×10^{-5}, and 9×10^{-5} cal/(cm · s · K); $B_{\lambda i} = 1 \times 10^{-8}$, 2.5×10^{-8}, and 5×10^{-8} cal/(cm · s · K^2); $A_{ci} = 0.2$, 0.25, and 0.3 cal/g · K; and $B_{ci} = 10^{-5}$, 5×10^{-5}, and 9×10^{-5} cal/(g · K^2).

III. Intrinsic Stability of Self-Sustaining Combustion

When studying intrinsic stability of EMs self-sustaining combustion, within the framework of the Zeldovich–Novozhilov (ZN) approach, the phase transition in the EM combustion wave has been neglected. However, the problem may be easily formulated to take into account phase transition within the framework of the main idea of the phenomenological approach.[21]

Simple consideration of all existing phase transitions in EMs leads to very cumbersome expressions. Let us take advantage of that for some widely used EMs (such as RDX and HMX) the thermal effect of melting is several times higher than the sum of the effects due to change in the structure and neglect the latter. In this case, similar to the classical approach,[21] one may determine the limit of combustion stability at constant pressure in the dependence on parameters k and r (for the derivation see the Appendix). The stability limit is a function of the $\bar{Q}_m$, $\bar{\lambda}$, and ϑ_m parameters. Convenient definitions are

$$k = (T_s - T_0) \left(\frac{\partial \ln r_b}{\partial T_0} \right)\Bigg|_P, \qquad r = \left(\frac{\partial T_s}{\partial T_0} \right)\Bigg|_P$$

$$\bar{Q}_m = \frac{Q_m}{c(T_s - T_0)}, \qquad \bar{\lambda} = \frac{\lambda_{\mathrm{sol}}}{\lambda_{\mathrm{liq}}}, \qquad \vartheta_m = \frac{T_m - T_0}{T_s - T_0}$$

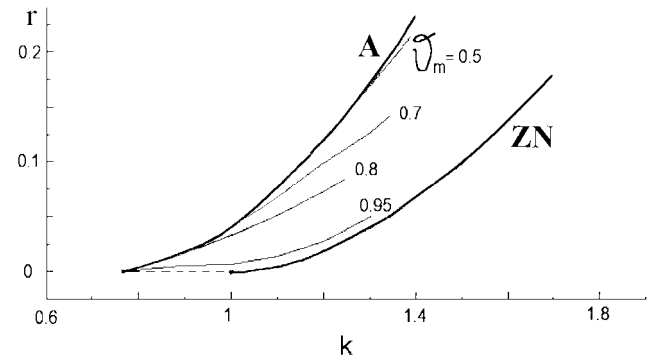

Fig. 1 Combustion stability limit for different values of ϑ_m ($\bar{Q}_m = 0.3$; $\bar{\lambda} = 1$) with curve A: $r = [k(1 + \bar{Q}_m) - 1]^2/[k(1 + \bar{Q}_m) + 1]$ and curve ZN: $r = (k-1)^2/(k+1)$.

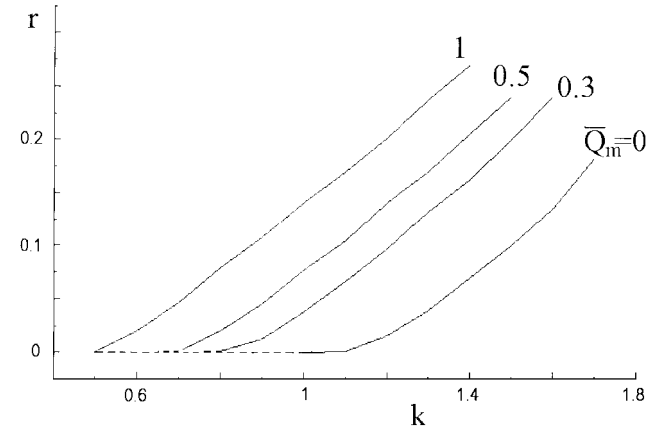

Fig. 2 Combustion stability limits for different values of $\bar{Q}_m$ ($\vartheta_m = 0.7$; $\bar{\lambda} = 1$).

Figure 1 shows the stability limit at $\bar{\lambda} = 1$ and $\bar{Q}_m = 0.3$ for different values of ϑ_m. The stability domain is located above the solid line. The calculated stability boundaries are between two limiting curves A and ZN for all k values. When this result is compared with that of the classical approach[21] stating stability limit at $r = (k-1)^2/(k+1)$, it becomes obvious that melting decreases stability.

The result obtained for relatively small values of k and r is important. It shows the possibility of combustion instability for melted EM at $k < 1$. Note that according to Ref. 21 the combustion without melting is unambiguously stable at $k < 1$.

Figure 2 shows the stability limit at $\bar{\lambda} = 1$ and $\vartheta_m = 0.7$ for various values of $\bar{Q}_m$. It is seen that when $\bar{Q}_m$ increases, the stability boundary shifts to the left of basic line ($\bar{Q}_m = 0$), which means that a domain of stable combustion becomes smaller in size.

A general character of the dependence of the stability limit position on the $\bar{Q}_m$ and ϑ_m parameters is shown in Fig. 3 in coordinates k^* and r, where $k^* = (T_s - T_0 + Q_m/c)\partial \ln r_b/\partial T_0 = k(1 + \bar{Q}_m)$. With this coordinate transformation, all curves originate from the point (1, 0). It is seen that the smaller the ϑ_m value on the line examined, the larger the distance between the origin of coordinates and branching from the basic line $r = (k^* - 1)^2/(k^* + 1)$. The magnitude of the curve $r(k^*)$ deviation from the basic line has a positive dependence on $\bar{Q}_m$.

The observed behavior of the curves has a simple physical meaning. Note that the temperature profile in the bulk of the condensed phase displays a peculiarity due to the phase transition only at the distance x_m from the burning surface. When $0 < x < x_m$, the Mikhelson profile is realized in the steady-state regime, which coincides with that for EM without phase transitions but with reduced initial temperature $T_0^* = T_0 - Q_m/c$. It is easy to calculate that $x_m = [\lambda_{\mathrm{liq}}/(r_b c_{\mathrm{liq}} \rho_{\mathrm{liq}})] \ln[(1 + \bar{Q}_m)/(\vartheta_m + \bar{Q}_m)]$. Note also that the harmonic thermal perturbations propagating with frequency $\omega \sim f$ in the bulk of EMs practically decay at a distance $x_{\mathrm{tw}} \sim 1/\sqrt{f}$.

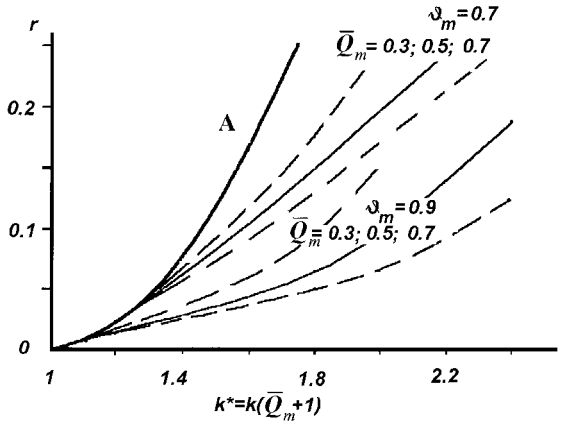

Fig. 3 Combustion stability limits in modified coordinates with curve A: $r = (k^* - 1)^2/(k^* + 1)$.

Obviously, with $x_{tw} < x_m$ the model is insensitive to phase transitions. For EMs without phase transitions, the results of Ref. 21 hold. Therefore, with $x_{tw} < x_m$, the stability limit coincides with $r = (k^* - 1)^2/(k^* + 1)$. As the melting temperature decreases, the thickness of the melted layer x_m increases. To preserve the equality $x_m = x_{tw}$, the branching point must be shifted along the basic line toward lower frequencies that is, far from the origin of the coordinates.

Consider now the case of fairly low perturbation frequencies when the characteristic distance of thermal wave decay x_{tw} becomes larger than the thickness of melted layer x_m. It means that perturbations reach the surface of phase transition. According to the Le Chatelier principle, this must strengthen the decay of perturbations more when the heat of the phase transition is larger. As a result, increase of $\bar{Q}_m$ leads to increase of the stability domain at $\vartheta_m = \text{const}$ in coordinates r and $k^* = k(1+\bar{Q}_m)$. This result reflects the dual nature of the effect of melting heat on the combustion stability. At arbitrary melting temperature, finite melting heat leads to the decrease of the stability domain caused by the effective decrease of the initial temperature. One may recognize this effect in Figs. 1 and 2 when analyzing the position of the beginning ($r = 0$) of curve A. At the same time, with the given value of melting temperature, when the temperature profile oscillations reach the liquid–solid interface, the melting heat acts as a damper and plays a positive role in increasing combustion stability in the plane r–k^* (see Fig. 3). However, this does not change the overall conclusion about the total negative effect of melting heat on combustion stability because of the predominant influence of the first factor. Note that calculations at $r \to 0$ (the region of high frequencies, see Figs. 1–3) require special analysis to take into account finite transition times in the gas phase and in the condensed phase reaction zone.[22]

IV. Burning Rate Response to Variations in Pressure

It is important from a practical point of view to predict the EM combustion behavior under pressure variations in order to estimate the possible growth of acoustic oscillations in the combustion chamber. The burning rate responses have been calculated for reference parameters selected according to published data[5–8] and with provision of coincidence with experimental data on RDX burning rate over the pressure range 1–90 atm. The reference parameters are listed in Table 1.

The calculated results for $R_p = (\Delta r_b/r_b)/(\Delta p/p)$ at 70-atm pressure are presented in Fig. 4. It is seen that the magnitude of the maximum of the pressure-driven burning rate response function decreases with the increase of melting temperature and the corresponding decrease of the melted layer width. A qualitative explanation of such behavior may be made as follows. According to the Le Chatelier principle, a phase transition (melting) diminishes the amplitude of oscillations of the thermal profile, but it works only at frequencies not exceeding a certain limiting value. The lower the melting temperature, the wider the melted layer is and the lower the limiting frequency is. The reason why the curve 1 in Fig. 4 has a relatively small maximum is that the melted layer is very narrow at $T_m = 580$ K.

Table 1 Reference parameters for EM physicochemical properties

Parameter	Value
Thermal conductivity	$\lambda_{liq} = \lambda_{sol} = 0.00055$ cal/(cm s K)
Specific heat of condensed phase	$C_{sol} = C_{liq} = 0.3$ cal/g K
Density of condensed phase	$\rho_{sol} = \rho_{liq} = 1.72$ g/cm^3
Latent heat of evaporation	$L = 112$ cal/g
Latent melting heat	$Q_m = 38$ (or 60) cal/g
Melting temperature	$T_m = 480$ (or 580) K
Boiling temperature at atmospheric pressure	$T_b = 613$ K
Initial temperature	$T_0 = 300$ K
Condensed phase Arrhenius activation energy	$E_{liq} = 47{,}100$ cal/mol
Condensed phase reaction heat	$Q_{liq} = 613$ cal/g
Gas phase Arrhenius activation energy	$E_1 = 15{,}500$ cal/mol and $E_2 = 50{,}000$ cal/mol
Gas phase reaction heat	$Q_1 = 725$ cal/g and $Q_2 = 235$ cal/g
Gas reaction order	$N_1 = 1.6$ and $N_2 = 1.6$
Pre-exponential factor	$A_{liq} = 10^{18.3}$ 1/s, $A_{g1} = 10^{10.2}$ g/(cm^3 s atm^{N_1}), $A_{g2} = 10^{10.2}$ g/(cm^3 s atm^{N_2})
Molecular mass of vapor	$M_1 = 222$ g/mol
Molecular mass of decomposition products	$M_2 = 35$ g/mol
Molecular mass of combustion products	$M_3 = 30$ g/mol

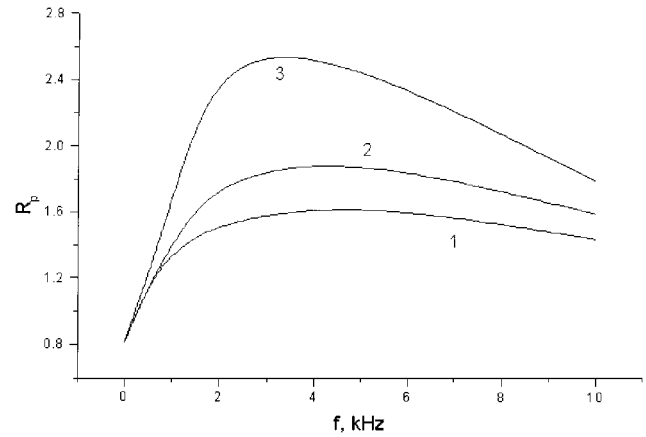

Fig. 4 Response function R_p vs frequency of pressure oscillations (p = 70 atm, $\Delta p/p = 0.02$) with 1: $T_m = 580$ K, $Q_m = 38$ cal/g; 2: $T_m = 480$ K, $Q_m = 38$ cal/g; and 3: $T_m = 480$ K, $Q_m = 60$ cal/g.

Comparison of curves 2 and 3 (Fig. 4) indicates that increase of melting heat leads to the loss of combustion stability, which is in agreement with the results of analysis of intrinsic combustion stability.

Analyzing Fig. 4 one may see that the behavior of burning rate response function at high frequencies does not follow the classical pattern with the diminishing response function magnitude to an infinitely small value. Instead, it is seen that at high frequencies the response function reaches a finite magnitude. A similar result was reported earlier in Ref. 21 for the common case when one does not use an assumption of existence of unambiguous correlation between surface temperature and burning rate. A simple qualitative explanation of the result discussed follows from the theory of heat propagation that states that the amplitude of oscillations of surface temperature diminishes to zero at high frequencies of oscillating heat feedback to the solid. In the case when the relationship $r_b = r_b(T_s)$ holds, this leads to diminishing amplitude of oscillations of the burning rate. However, in the common case when such correlation does not exist, the finite amplitude oscillations of r_b at high frequencies are possible.

V. Summary and Conclusions

The results of this study show that the effect of melting on the combustion behavior of EM can be qualitatively explained from the

point of view of classic thermal theory of combustion. If one assumes that the increase in absolute value of the melting heat is equivalent to the decrease of initial temperature of EMs, the observed decrease of intrinsic combustion stability in response to small or finite pulse perturbations of heat flux is the result of lowering the effective initial temperature. The influence of initial temperature on the combustion stability limit is determined by the closeness of calculated value of parameter $k = (T_s - T_0)(\partial \ln r_b/\partial T_0)_p$ to its critical value, corresponding to the boundary of stable combustion regimes. In the case of gas phase reactions controlling the propellant burning rate, the coefficient $\partial \ln r_b/\partial T_0 \sim E_g/RT_g^2$ has a weak dependence on T_0 and parameter k increases when initial temperature T_0 decreases. Thus, with T_0 decreasing, the combustion stability becomes lower due to the increase of parameter k. This statement works in the case of small perturbations and may work in the case of finite amplitude perturbations.

The effect of the magnitude of the melting temperature can be qualitatively treated through the analysis of the interaction of thermal disturbances with melting surface. When the thermal wave penetrates deep into the bulk of EMs and reaches the melting surface, the interaction with the heat sink caused by the EM melting leads to the weakening (dissipation) of the thermal disturbance as follows from the Le Chatelier principle. Therefore, the higher the melting temperature (closer to the burning surface temperature), the higher is the stability of transient combustion.

Calculations within the framework of the proposed mathematical model for combustion of melted and evaporated EMs showed that variations of the surface temperature are effectively reduced by surface heat sink created by EM evaporation. This leads to the relatively small magnitude of parameter $r = (\partial T_s/\partial T_0)_p$ and to the relatively weak frequency dependence of burning rate response to pressure oscillations. It should be noted that such theoretical predictions still have no actual confirmation in experiments.

To conclude, in the present work the influence of the melting heat and the melting temperature on the combustion behavior of EMs on self-sustaining combustion and under harmonic pressure variations has been studied. It is shown that increase of heat loss on melting decreases the intrinsic stability of self-sustaining combustion and dynamic combustion under harmonic pressure variations. The increase of melting temperature increases stability of self-sustaining combustion.

In the future research, it would be useful to study the combustion behavior of EMs with pressure drop. Preliminary calculations with different depressurization times showed that the boundary of stable transition to the lower pressure combustion regime has a more complicated character, as was expected. It is also of interest to study the peculiarities of radiation-driven transient combustion of melted and evaporated EMs. In addition, the possible effects of thermally induced mechanical deformations on the combustion behavior of crystalline melted EMs have to be estimated.

Appendix: Equation for the Combustion Stability Boundary

Similar to Ref. 21, the problem is reduced to the analysis of the solution of the thermal conductivity equation in the system of coordinates attached to the surface. That at temperature $T = T_m$ the melting is followed by both the thermal effect $-Q_m$ and the change in the coefficient of thermal conductivity (with $T < T_m$, $\lambda = \lambda_{\text{sol}}$ and with $T > T_m$, $\lambda = \lambda_{\text{liq}}$) is taken into account.

Introducing the dimensionless parameters

$$\vartheta = \frac{T - T_0}{T_s^0 - T_0}, \qquad \xi = x r_b^0 \left(\frac{C\rho}{\lambda}\right)_{\text{sol}}, \qquad H = x_m r_b^0 \left(\frac{C\rho}{\lambda}\right)_{\text{sol}}$$

$$\tau = t\left(r_b^0\right)^2 \left(\frac{C\rho}{\lambda}\right)_{\text{sol}}, \qquad \bar{r}_b = \frac{r_b}{r_b^0}, \qquad \bar{\lambda} = \frac{\lambda_{\text{sol}}}{\lambda_{\text{liq}}}$$

$$\bar{Q}_m = \frac{Q_m}{C\left(T_s^0 - T_0\right)}$$

the problem takes the form

$$\frac{\partial \vartheta}{\partial \tau} - \bar{r}_b \frac{\partial \vartheta}{\partial \xi} = \frac{1}{\bar{\lambda}} \frac{\partial^2 \vartheta}{\partial \xi^2}, \qquad 0 < \xi < H$$

$$\vartheta(0, \tau) = \vartheta_s(\varphi), \qquad \bar{r}_b = \bar{r}_b(\varphi), \qquad \varphi = \frac{\partial \vartheta}{\partial \xi}(0, \tau)$$

$$\frac{\partial \vartheta}{\partial \tau} - \bar{r}_b \frac{\partial \vartheta}{\partial \xi} = \frac{\partial^2 \vartheta}{\partial \xi^2}, \qquad \vartheta(\infty, \tau) = 0, \qquad \vartheta(H(\tau), \tau) = \vartheta_m$$

$$H(\tau) < \xi < \infty$$

$$\frac{1}{\bar{\lambda}} \frac{\partial \vartheta}{\partial \xi}\bigg|_{H-0} = \frac{\partial \vartheta}{\partial \xi}\bigg|_{H+0} - \bar{Q}_m \bar{V}_m, \qquad \bar{V}_m = \frac{\mathrm{d}H}{\mathrm{d}\tau} + \bar{r}_b$$

Here the variability of $C\rho$ is neglected; the superscript 0 and subscripts 0, s, and m refer to the steady-state regime, the initial state, the surface, and the melting point. The functions $\vartheta_s(\varphi)$ and $r_b(\varphi)$ are assumed to be known from either experiment or steady-state regime calculations. The stationary solution to the system has the form

$$\vartheta^0 = 1 - (1 - \vartheta_m)\frac{1 - \exp(-\bar{\lambda}\xi)}{1 - \exp(-\bar{\lambda}H)}, \qquad 0 < \xi < H$$

$$\vartheta^0 = \vartheta_m e^{-(\xi - H)}, \qquad H < \xi < \infty$$

$$H = \frac{1}{\bar{\lambda}} \ln A, \qquad A = \frac{\bar{Q}_m + 1}{\bar{Q}_m + \vartheta_m}$$

Let us linearize the problem in the vicinity of the steady-state regime assuming that

$$\vartheta = \vartheta^0 + \delta\vartheta(\xi) e^{\omega\tau}, \qquad \bar{r}_b = 1 + \delta\bar{r}_b e^{\omega\tau}$$

$$H = H^0 + \delta H e^{\omega\tau}, \qquad \omega = 2\pi f (\lambda/C\rho)_{\text{sol}} \Big/ \left(r_b^0\right)^2$$

After linearization we get the system of equations

$$\omega\delta\vartheta + \delta\bar{r}_b \bar{\lambda} \frac{1 - \vartheta_m}{1 - e^{-\bar{\lambda}H}} e^{-\bar{\lambda}\xi} - \frac{\mathrm{d}\delta\vartheta}{\mathrm{d}\xi} = \frac{1}{\bar{\lambda}} \frac{\mathrm{d}^2\delta\vartheta}{\mathrm{d}\xi^2}, \qquad 0 < \xi < H \tag{A1}$$

$$\omega\delta\vartheta + \delta\bar{r}_b \vartheta_m e^{-(\xi - H)} - \frac{\mathrm{d}\delta\vartheta}{\mathrm{d}\xi} = \frac{\mathrm{d}^2\delta\vartheta}{\mathrm{d}\xi^2}, \qquad H < \xi < \infty \tag{A2}$$

When solving the system, we do not use boundary conditions in the Eq. (A1) case that leads to the appearance of undetermined constants D_1 and D_2. Solution of Eq. (A2) is found using conditions $\delta\vartheta(\infty) = 0$ and $-\vartheta_m \delta H + \delta\vartheta(H) = 0$,

$$\delta\vartheta = (\bar{Q}_m + \vartheta_m)\left[-\delta\bar{r}_b(\bar{\lambda}/\omega)e^{-\bar{\lambda}(\xi - H)} + D_1 e^{-k_1\bar{\lambda}\xi} + D_2 e^{-k_2\bar{\lambda}\xi}\right]$$

$$0 < \xi < H$$

$$\delta\vartheta = -(\vartheta_m/\omega)\delta\bar{r}_b e^{-(\xi - H)} + \vartheta_m e^{-k_3(\xi - H)}[\delta H + (1/\omega)\delta\bar{r}_b]$$

$$H < \xi < \infty$$

$$k_1 = 0.5\left(1 + \sqrt{1 + 4\omega/\bar{\lambda}}\right), \qquad k_2 = 1 - k_1$$

$$k_3 = 0.5\left(1 + \sqrt{1 + 4\omega}\right)$$

The preceding solutions provide useful relationships,

$$\delta\vartheta|_0 = (\bar{Q}_m + \vartheta_m)[-\delta\bar{r}_b(\bar{\lambda}/\omega)A + D_1 + D_2] \tag{A3}$$

$$\frac{\mathrm{d}\delta\vartheta}{\mathrm{d}\xi}\bigg|_0 = (\bar{Q}_m + \vartheta_m)\bar{\lambda}\left[\delta\bar{r}_b \frac{\bar{\lambda}}{\omega} A - k_1 D_1 - k_2 D_2\right] \tag{A4}$$

$$\delta\vartheta|_{H-0} = (\bar{Q}_m + \vartheta_m)\left[-\delta\bar{r}_b(\bar{\lambda}/\omega) + D_1 A^{-k_1} + D_2 A^{-k_2}\right] \tag{A5}$$

$$\left.\frac{d\delta\vartheta}{d\xi}\right|_{H-0} = (\bar{Q}_m + \vartheta_m)\bar{\lambda}\left(\delta\bar{r}_b\frac{\bar{\lambda}}{\omega} - k_1 D_1 A^{-k_1} - k_2 D_2 A^{-k_2}\right) \quad \text{(A6)}$$

$$\left.\frac{d\delta\vartheta}{d\xi}\right|_{H+0} = \vartheta_m\left[\frac{1}{\omega}\delta\bar{r}_b - k_3\left(\delta H + \frac{1}{\omega}\delta\bar{r}_b\right)\right] \quad \text{(A7)}$$

$$\left.\frac{d\vartheta^0}{d\xi}\right|_0 = -\bar{\lambda}(\bar{Q}_m + 1) \quad \text{(A8)}$$

$$\left.\frac{d\vartheta^0}{d\xi}\right|_{H-0} = -\bar{\lambda}(\bar{Q}_m + \vartheta_m) \quad \text{(A9)}$$

$$\left.\frac{d^2\vartheta^0}{d\xi^2}\right|_{H-0} = \bar{\lambda}^2(\bar{Q}_m + \vartheta_m) \quad \text{(A10)}$$

$$\left.\frac{d^2\vartheta^0}{d\xi^2}\right|_{H+0} = \vartheta_m \quad \text{(A11)}$$

Let us take into account four linearized boundary conditions that were not yet used,

$$\delta\vartheta|_{H-0} = -\delta H\left.\frac{d\vartheta^0}{d\xi}\right|_{H-0}$$

$$\frac{1}{\bar{\lambda}}\left(\delta H\left.\frac{d^2\vartheta^0}{d\xi^2}\right|_{H-0} + \left.\frac{d\delta\vartheta}{d\xi}\right|_{H-0}\right) = \delta H\left.\frac{d^2\vartheta^0}{d\xi^2}\right|_{H+0} + \left.\frac{d\delta\vartheta}{d\xi}\right|_{H+0}$$

$$- \bar{Q}_m(\delta\bar{r}_b + \omega\delta H)$$

$$\delta\overline{r_b} = \frac{k^*}{k^* + r - 1}\frac{d\delta\vartheta}{d\xi}(0)\Big/\frac{d\vartheta^0}{d\xi}(0)$$

$$\delta\vartheta(0) = \frac{r}{k^*}\delta\bar{r}_b(1 + \bar{Q}_m)$$

The equation of stationary thermal balance, $\lambda_{sol}\partial T/\partial x = (C\rho)_{sol} r_b(T_s - T_0 + Q_m/C_{sol})$, differentiated with respect to parameter T_0 was used on linearization. Substituting expressions (A3–A11) for the values included into the four boundary conditions, we get four linear equations for δH, $\delta\bar{r}_b$, D_1, and D_2 with the right-hand sides equal to zero. Thus, a corresponding determinant must be equal to zero. It depends on the parameters ω, r, k^*, ϑ_m, $\bar{Q}_m$, and $\bar{\lambda}$. Assuming that $\omega = i\bar{\lambda}s$ and $i = \sqrt{-1}$, we obtain a complex determinant. By equating it to zero for the fixed ϑ_m, $\bar{Q}_m$, and $\bar{\lambda}$, a parametric (with parameter s) dependence $r(k^*)$ at the boundary of the oscillating instability of the initial problem solution to the action of small perturbations is derived. Simplifying the determinant, we get the representation of the boundary in the form

$$B \equiv |b_{n,j}| = 0, \qquad b_{1,1} = 0, \qquad b_{1,2} = k^* + isr, \qquad b_{1,3} = 1$$

$$b_{1,4} = 1, \qquad b_{2,1} = 0, \qquad b_{2,2} = k^* + is(r + k^* - 1)$$

$$b_{2,3} = k_1, \qquad b_{2,4} = k_2, \qquad b_{3,1} = 1, \qquad b_{3,2} = 0$$

$$b_{3,3} = A^{-k_1}, \qquad b_{3,4} = A^{-k_2}$$

$$b_{4,1} = 1 + is + \frac{\vartheta_m}{\bar{Q}_m + \vartheta_m}\frac{4s^2\bar{\lambda}}{\left(1 + \sqrt{1 + 4is\bar{\lambda}}\right)^2}$$

$$b_{4,2} = 0, \qquad b_{4,3} = k_1 A^{-k_1}, \qquad b_{4,4} = k_2 A^{-k_2}$$

Solution to the $\mathrm{Re}(B) = 0$, $\mathrm{Im}(B) = 0$ system using the Mathcad 3 computer code is given in Figs. 1–3.

Acknowledgments

The authors thank the Russian Foundation for Basic Research (Grant 97-01-00860) and International Association for the Promotion of Cooperation with Scientists from the New Independent States of the Former Soviet Union (INTAS) (Grant 93-2560-ext) for support of this study.

References

[1] Alexandrov, V. V., Gladkikh, V. M., and Khlevnoi, S. S., "Thermal Decomposition of a Mixture Based on Ammonium Perchlorate," *Combustion, Explosion, and Shock Waves*, Vol. 5, No. 4, 1969, pp. 581, 582.

[2] Zarko, V. E., Gusachenko, L. K., and Rychkov, A. D., "Simulation of Combustion of Melting Energetic Materials," *Defence Science Journal* (India), Vol. 46, No. 5, 1996, pp. 425–433.

[3] Gusachenko, L. K., "Effect of Melting on Combustion Stability of Quasi-homogeneous Compositions. The Zeldovich–Novozhilov Method," *Combustion, Explosion, and Shock Waves*, Vol. 34, No. 4, 1998, pp. 26–29.

[4] Cozzi, F., De Luca, L., and Novozhilov, B. V., "Linear Stability and Pressure-Driven Response Function of Energetic Solid Materials with Phase Transition," *Journal of Propulsion and Power* (submitted for publication).

[5] Bizot, A., and Beckstead, M. W, "Role of Carbon/Carbonageous Matter Formation in the Combustion of Double Base Rocket Propellants," *Flame Structure*, Vol. 1, Nauka, Novosibirsk, Russia, 1991, pp. 230–235.

[6] Kuo, K. K., and Lu, Y.-C., "Modeling of Physicochemical Processes of RDX Monopropellant with Detailed Treatments for Surface Reaction Zone," *Challenges in Propellants and Combustion 100 Years After Nobel*, edited by K. K. Kuo et al., Bergel House, New York, 1997, pp. 583–600.

[7] Rogers, R. N., and Daub, G. W., *Analytical Chemistry*, Vol. 45, No. 3, 1973, pp. 596–600.

[8] Melius, C. F., "Thermochemical Modeling: II. Application to Ignition and Combustion of Energetic Materials," *Chemistry and Physics of Energetic Materials*, edited by S. N. Bulusu, NATO ASI Series, Kluwer Academic, Norwell, MA, 1990, pp. 51–78.

[9] Liau, Y.-C., and Yang, V., "Analysis of RDX Monopropellant Combustion with Two-Phase Subsurface Reactions," *Journal of Propulsion and Power*, Vol. 11, No. 4, 1995, pp. 729–739.

[10] Davidson, J., and Beckstead, M., "Improvements to RDX Combustion Modeling," AIAA Paper 96-0885, Jan. 1996.

[11] Ermolin, N. E., and Zarko, V. E., "Reduction of Kinetic Mechanism for RDX Combustion," *Combustion, Explosion, and Shock Waves*, 1999 (submitted for publication).

[12] Margolin, A. D., and Pokhil, P. F., *Doklady Akademii Nauk SSSR*, Vol. 150, No. 6, 1963, pp. 1304–1306.

[13] Yakusheva, O. B., Maksimov, E. I., and Merzhanov, A. G., "The Effect of Gaseous Decomposition Products Solubility on the Condensed Substances Burning Regularity," *Combustion, Explosion, and Shock Waves*, Vol. 2, No. 3, 1966, pp. 125–129.

[14] Maksimov, E. I., and Merzhanov, A. G., "To the Theory of the Condensed Systems Combustion," *Combustion, Explosion, and Shock Waves*, Vol. 2, No. 1, 1966, pp. 47–58.

[15] Margolis, S. B., Williams, F. A., and Armstrong, R. C., "Influences of Two-Phase Flow in the Deflagration of Homogeneous Solids," *Combustion and Flame*, Vol. 67, No. 3, 1987, pp. 249–258.

[16] Li, S. C., Williams, F. A., and Margolis, S. B., "Effects of Two-Phase Flow in a Model for Nitramine Deflagration," *Combustion and Flame*, Vol. 80, No. 3, 1990, pp. 329–349.

[17] Margolis, S. B., and Williams, F. A., "Effect of Two-Phase Flow on the Deflagration of Porous Energetic Materials," *Journal of Propulsion and Power*, Vol. 11, No. 4, 1995, pp. 759–768.

[18] Zarko, V. E., Zyryanov, V. Y., and Chertischev, V. V., "Dispersion of the Surface Layer During Combustion of Homogeneous Propellants," AIAA Paper 96-0814, Jan. 1996.

[19] Ben-Reuven, M., and Caveny, L. H., "Nitramine Flame Chemistry and Deflagration Interpreted in Terms of a Flame Model," *AIAA Journal*, Vol. 19, No. 10, 1981, pp. 1276–1285.

[20] Brill, T. B., "Multiphase Chemistry Considerations at the Surface of Burning Nitramine Monopropellants," *Journal of Propulsion and Power*, Vol. 11, No. 4, 1995, pp. 740–751.

[21] Novozhilov, B. V., *Nonstationary Combustion of Solid Propellants*, Nauka, Moscow, 1973; also Translation AFSC FTD-MT-24-317-74.

[22] Novozhilov, B. V., "Influence of Thermal Gas Phase Inertia on Combustion Stability of Evaporating Condensed Systems," *Khimitcheskaya Fizika*, Vol. 7, No. 3, 1988, pp. 388–396.